



Doped Mott-Hubbard materials with a low quasiparticle transparency

V. A. Gavrichkov 

*Kirensky Institute of Physics, Siberian Branch of the Russian Academy of Sciences, 660036 Krasnoyarsk, Russia
and Rome International Center for Materials Science Superstripes RICMASS, via del Sabelli 119A, 00185 Roma, Italy*

 (Received 19 November 2023; revised 20 February 2024; accepted 21 February 2024; published 21 March 2024)

Based on the Wilson's criterion metal/insulator, extended to materials with strong electronic correlations, we have identified a specific class of the materials, which is not associated with their usual classification into Mott-Hubbard and charge transfer dielectrics. The local symmetry of these materials leads to the disappearance of quasiparticle states (so-called first removal or first extra states) in the Hubbard gap. It is especially unusual for doped materials, in which quasiparticles, being charge carriers, can disappear or appear under external factors without the Mott transition being achieved. In this work, we introduce the so-called "quasiparticle transparency", and provide specific experiments to identify materials with the low quasiparticle transparency. A number of examples of such materials with a spin crossover under high pressure, showing the Jahn-Teller nature, are considered.

DOI: [10.1103/PhysRevB.109.125139](https://doi.org/10.1103/PhysRevB.109.125139)

I. INTRODUCTION

The satisfiability of the known metal/insulator (MI) criterion $W/U \sim (R + 1)$ (where R is the orbital degeneracy) of the Mott-Hubbard transition depends on the characteristic material scale, since the width W of the quasiparticle band decreases with the decreasing scale of materials, and the Coulomb interaction U increases due to the weakening of screening effects. The MI transition itself can also be controlled by external effects, which change physical properties of the material (thermal expansion, pressure, optical pumping, etc.). Of particular interest is the transition of Mott-Hubbard insulators to a metallic state induced by the doping effect, since doped materials have unique properties, e.g., high temperature superconductivity in the two-dimensional (2D) perovskite cuprates [1,2] and colossal magnetoresistance in 3D manganites [3,4]. Moreover, in both materials the pseudogap effect is observed. However, it is hard to imagine that the initial MI criterion is correct in all these various cases.

To understand the origin of the problem, it is sufficient to look at the "band structure" within the framework of the formalism of Hubbard operators [5] in the zero-hopping approximation. The formalism is necessary to detect the effects of many-electron local states on the number of quasiparticles in the band. In the zero-hopping approximation, according to the initial MI criterion, the material must be an insulator ($W = 0$), but the MI criterion based on Wilson's ideas [6] for the doped Mott-Hubbard materials shows nontrivial scale invariant results, independent of the band width W . The purpose of our work is to construct and apply Wilson's MI criterion as related to the system of itinerant electrons in the analytical form to the doped Mott-Hubbard materials. The approach includes a key statement that if an electron system consists of completely occupied and empty bands, it is an insulator, otherwise, it is a metal, where however the spectral density of quasiparticles depends

on the doped carrier concentration x due to many-electron effects.

II. WILSON'S MI CRITERION FOR DOPED MATERIALS

To extend the Wilson's MI criterion, we will further follow the work [7] where it is demonstrated that doped 2D perovskite cuprates have metallic conductivity, with no forbidden quasiparticle states being present. Although there are some features here (e.g., an impurity potential effect and associated states), we will consider the criterion taking into account the many-electron effects only. Our extended approach uses the fact that the optical intracell dd transitions with their (l orbital, S spin)-selection rules in the transparency window and optical charge transfer transitions in the oxides can be observed in the same $3d$ states [8,9]. Note, in order to make further content more self-sufficient, we have also provided here some calculation details from Ref. [7] (see Appendix A).

In the first approximation we can assume that the quasiparticles are unit cell excitations which can be represented graphically as single-particle transitions between different sectors $N_h = \dots(N_{h0} - 1), N_{h0}, (N_{h0} + 1), \dots$ of the configuration space of the unit cell (N_{h0} -hole number per cell in the undoped material, see Fig. 1) [10]. Each of these transitions forms an r th quasiparticle band, where the root vector $r = \{ii'\}$ in the configuration space numerates the initial i and final i' many-electron states in the transition. The quasiparticle transitions with increasing or decreasing electrons form the conduction or valence bands, respectively. The indices i and i' run over multi-electron states: $\mu, \tau, \text{ and } \eta$ in the sectors $N_{h0}, N_{h0} - 1$ and $N_{h0} + 2$ (see Fig. 1). Here, it is convenient to start with Lehmann representation of the Green's function $G_{f\sigma}^{\lambda\lambda}$ of the intracell Hamiltonian H_0 with respect to the family of single-particle operators $c_{f\lambda\sigma}^{(+)}$ with the $f(g)$ cell, λ orbital, $\sigma = \uparrow, \downarrow$ spin indices, and their matrix elements in the basis of $|(N_h, M_S)_i\rangle$ eigenstates of H_0 (S and M spin and spin

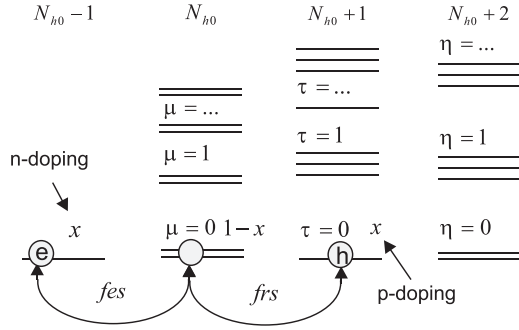


FIG. 1. $E_i(N_h, M_S)$ -energy level scheme of the configuration space based on the cell states with hole number per cell $N_h = N_{h0} - 1, N_{h0}, N_{h0} + 1, \dots$, where $i = \mu, \tau, \eta$ and N_{h0} is the hole number per cell in the undoped material. The circles e and h denote the occupied ground cell states of the electron- and hole-doped materials, respectively. The solid line with arrows corresponds to the first extra states (fes) and first removal state (frs) quasiparticles.

projection of the multielectron cell eigenstate):

$$\begin{aligned} \sum_{\lambda\sigma} G_{fg\sigma}^{\lambda\lambda} &= \sum_{\lambda\sigma} \langle \langle c_{f\lambda\sigma} | c_{g\lambda\sigma}^+ \rangle \rangle \\ &= \delta_{fg} \sum_{rr'} \sum_{\lambda\sigma} \gamma_{f\lambda\sigma}(r) \gamma_{f\lambda\sigma}(r') D_{fg}^{rr'}(E) \\ &= \delta_{fg} \sum_{rr'} \delta_{rr'} \sum_{\sigma} \frac{F_r(x) \chi_{rr}^{\sigma}}{E - \Omega_r^{\sigma}}, \end{aligned} \quad (1)$$

where matrix elements

$$\begin{aligned} \gamma_{\lambda\sigma}(r) &= \langle (N_h + 1, M'_S)_{\tau} | c_{f\lambda\sigma} | (N_h, M_S)_{\mu} \rangle \\ &\times \delta(S', S \pm |\sigma|) \delta(M', M + \sigma), \end{aligned} \quad (2)$$

and

$$\chi_{rr'}^{\sigma} = \sum_{\lambda} \gamma_{\lambda\sigma}^*(r) \gamma_{\lambda\sigma}(r') \quad (3)$$

for the p - and n -quasiparticle states in the valence and conduction bands, respectively, where the total space of the root vectors $\{r\} = \dots + \{r_{12}\} + \{r_{23}\} + \dots$, $\{r_{12}\} = \{\mu\tau\}$, $\{r_{23}\} = \{\tau\eta\}$ and so on (see Fig. 1). The occupation factor $F_r(x)$ is the probability to detect a cell in any of the i, i' states participating in the r th transition, and $\Omega_r^v = E_i(N_h, M_S) - E_{i'}(N_h + 1, M'_S)$ and $\Omega_r^c = E_i(N_h - 1, M_S) - E_{i'}(N_h, M'_S)$ are the quasiparticle energies in the r th valence and conduction bands, respectively. In the paramagnetic (PM) phase of the doped material the occupation factor has the form:

$$F_{r_{12}}(x) = \frac{1 - \alpha x}{2S + 1}, \quad (4)$$

where $\alpha = 1 - (2S + 1)/(2S' + 1)$ is proportional to the ratio of the spin multiplets of the i, i' states participating in the r_{12} -transition (from the subspace $\{r_{12}\}$) between the ground states $|(N_{h0}, M_S)_{i=0}\rangle$ and $|(N_{h0} + 1, M'_S)_{i'=0}\rangle$ indicated by the arrows in Fig. 1.

The Green's function in Eq. (1) is yet free from the shortcomings of the hydrogenlike representation and low-energy approximations since we do not restrict ourselves to choose

the intracell Hamiltonian H_0 , and are ready to work with all the $|(N_h, M_S)_i\rangle$ states. Taking into account the specifics of the cuprates, we will consider p -doped materials, where the number of valence states is equal to the sum over all quasiparticle states:

$$\begin{aligned} N_v(x) &= \sum_{\lambda\sigma} \sum_r \gamma_{\lambda\sigma}^2(r) \int dE \left(-\frac{1}{\pi} \right) \text{Im} D_0^i(E)_{E+i0} \\ &= N_v^{12}(x) + N_v^{23}(x), \end{aligned} \quad (5)$$

where $N_v^{12}(x)$ and $N_v^{23}(x)$ are the contributions from the quasiparticles with the root vectors r from the $\{r_{12}\}$ and $\{r_{23}\}$ subspaces since the other states of $|(N_h, M_S)_i\rangle$ in the p -doped material are not occupied, and there is a zero probability $F_r(x) = 0$ to detect a cell in these states at a low temperature. The Wilson's condition in the insulating state, which we are interested in, is

$$N_e - x = N_v(x), \quad (6)$$

where $(N_e - x)$ is the total electron number per cell of the hole doped material. That is, if the number of electrons in the cell equals the number of valence quasiparticle states, the doped material is an insulator.

To obtain the Fermi level position in a degenerate doped material at zero temperature we could perform the integration on the right side of the equation

$$x = \sum_{\lambda\sigma} \sum_r \gamma_{\lambda\sigma}^2(r) \int_{E_F} dE \left(-\frac{1}{\pi} \right) \text{Im} D_0^i(E)_{E+i0}, \quad (7)$$

over the top valence band of the first removal electron states (frs) with the lowest binding energy (see Fig. 1), and this is, as a rule, sufficient at the actual concentration $x \sim 0.1$. However, this is not sufficient, when the hole concentration x exceeds the number of quasiparticle states in the top valence band $x \gg N_{\text{frs}}$, since the number of the frs quasiparticle states, N_{frs} , may be very small. Therefore, the solution of Eq. (7) has the features at $N_{\text{frs}} \rightarrow 0$. To understand this, we obtain the total number of valence quasiparticle states, N_v , as a function of both the doping concentration x , and N_{frs} :

$$N_v(x, N_{\text{frs}}) = N_v^{12} + N_v^{23}, \quad (8)$$

where the contributions N_v^{12} and N_v^{23} from the subspaces $\{r_{12}\}$ and $\{r_{23}\}$ are calculated in Appendix A, and the root vectors r characterize the specific quasiparticle band: if $r = \{v_0, l_0\}$ or $r = \{\tau_0, l_0\}$ in Eqs. (2) and (3), then we are dealing with the first extra states (fes) or frs quasiparticles in Fig. 1, respectively. By following this approach, we obtain an MI criterion:

$$N_v(x) = N_e - x(1 - N_{\text{frs}}), \quad (9)$$

which is characterized by a condition: $N_{\text{frs}} = 0$ (insulator) or $N_{\text{frs}} \neq 0$ (metal), and N_{frs} is calculated in Appendix A. Indeed, under the conditions $N_{\lambda} = N_e = 1$ we always obtain a simple metal with the valence states $N_{\text{frs}} = 2$ and $N_v(x) = (1 + x)$, as it occurs in the Hubbard model, where the high-spin (triplet) states are simply not available. The criterion is based only on the properties of completeness of a set of states $|(N_h, M_S)_i\rangle$ in the configuration space of the cell, and the number of states N_{frs} depends on their spin and orbital nature.

III. QUASIPARTICLES IN DOPED MATERIALS WITH LOW QUASIPARTICLE TRANSPARENCY

From Eq. (9) it follows that the doped material can show both the metallic $N_v(x) > (N_e - x)$, and dielectric properties $N_v(x) = (N_e - x)$ at the $N_{\text{frs}} > 0$ or $N_{\text{frs}} = 0$, respectively. The physical meaning of the MI criterion lies in the matrix value $\chi_{rr'}^\sigma$ [see Eq. (3)], which in the Hubbard operator representation corresponds to the quasiparticle as a sequence of intracell transitions between the multielectron cell states. If single-particle transitions are forbidden by any symmetry, the charge carriers are missing. The doping particles (electrons or holes) are in the local multielectron states $|(N_h, M_S)_i\rangle$, but there is no peak in the single-particle density of states, and the matrix element $\chi_{r_0 r_0}^\sigma$ defined in the root vector space $\{r\}$ can be called ‘‘quasiparticle transparency’’ of the doped material.

A. Pressure-induced effects

The frs states can be prohibited at the $\delta(S', S \pm |\sigma|) = 0$ in Eqs. (2) and (3) (s -forbidden frs quasiparticles). However, can forbidden $frs(frfs)$ states really exist in any doped Mott-Hubbard materials? A review of the Tanabe-Sugano diagrams [11] shows that the low transparency effects in the materials with $3d$ elements in an octahedral environment are unlikely. Indeed, the ground states in different sectors of the configuration space are connected by nonzero matrix elements (2) of the single-particle operators. However, the nature of the ground state of the transition element ion depends on the applied pressure, while some materials with $3d^k$ ions at $3 < k < 8$, namely, the transition metal oxides, transition metal complexes, metal-organic molecules and molecular assemblies, exhibit spin crossover, with increasing pressure from ambient pressure [12–23]. The spin crossover occurs due to the competition between the energy crystal field $10Dq$ and the intra-atomic Hund exchange J_H , for example, in an interesting material FeBO_3 [24], where the Fe^{3+} ion is in the high-spin configuration $3d^5(t_{2g}^3 e_g^2)$ at ambient pressure. The energy of the high and low spin states in the $N_0(3d^5)$ sector can be presented in the form [25]:

$$\begin{aligned} E_{hs} &= E_c(d^5) - 10J_H \\ E_{ls} &= E_c(d^5) - 20Dq - 4J_H. \end{aligned} \quad (10)$$

Equation (10) shows that the spin crossover $S|_{P < P_S} = 5/2 \leftrightarrow S|_{P > P_S} = 1/2$ in the ground state is possible at a certain pressure P_S ($= 48 - 54$ GPa for iron borate [24]) corresponding to the crystal field $10Dq = 3J_H$. Here and below, E_c is a part of the energy term independent of the Hund exchange J_H and the crystal field $10Dq$ [26]. Similarly, in the sector N_+ for the $3d^6$ configuration

$$\begin{aligned} E_{hs} &= E_c(d^6) - 4Dq - 10J_H, \\ E_{ls} &= E_c(d^6) - 24Dq - 6J_H, \end{aligned} \quad (11)$$

for the spins $S_{v_0} = 2$ and $S_{v_0} = 0$, respectively. This shows that the crossover in the ground state of the term is possible, under the condition $10Dq = 2J_H$, in accordance with the pressure P_{min} . Similarly, in the sector N_- for the $3d^4$ configuration

$$\begin{aligned} E_{hs} &= E_c(d^4) - 6Dq - 6J_H, \\ E_{ls} &= E_c(d^4) - 16Dq - 3J_H. \end{aligned} \quad (12)$$

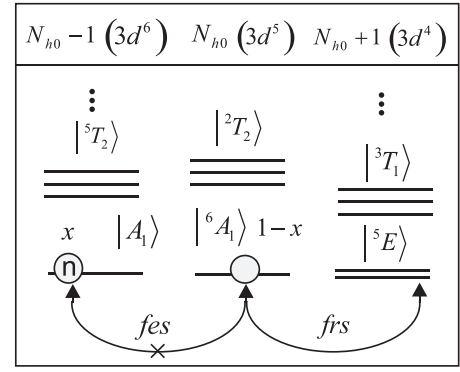


FIG. 2. Ground state crossover $S_{v_0} = 2 \leftrightarrow 0$ in the $N_{h_0} - 1$ sector FeBO_3 under the pressure $P_{\text{min}} < P < P_S$. The solid elliptical line with a cross shows the forbidden fes quasiparticles.

Equation (12) shows that the crossover in the ground state of the term is possible at the same crystal field $10Dq = 3J_H$ as for the $3d^5$ configuration. The energy of the ground states in Eqs. (10) and (12) in the pressure range $P_{\text{min}} < P < P_S$ promotes the forbidden fes quasiparticles (see Fig. 2), and the n -doped iron borate, can turn out to be an insulator (semiconductor), where

$$\chi_{r_0 r_0}^\sigma = \sum_{\lambda} \gamma_{\lambda\sigma}^*(^6A_1, ^5E) \gamma_{\lambda\sigma}(^5E, ^6A_1) = 0 \quad (13)$$

at $\delta(S' = 0, S = 5/2 \pm |\sigma|) \delta(M', M + \sigma) = 0$. The disappearance of n quasiparticles precedes the spin crossover at the pressure P_S . Note, however, that the iron borate has not so far been able to be converted into the metallic state with an increase in pressure. The similar calculations for all $3d^n$ ionic configurations in the octahedral crystal field show a possibility for the forbidden fes and frs quasiparticles only in the n -doped materials with $3d^5$ and the p -doped materials with $3d^6$ ions, respectively.

B. Quasiparticles induced by the pseudo-JT effect

The second possibility to observe the effects of low quasiparticle transparency is the material with the dynamic Jahn-Teller (JT) effect, where the hole doping changes the initial orbital configuration of the $|(N_{h_0}, M_S)_{\mu=0}\rangle$ ground cell states (l forbidden frs quasiparticles). Indeed, in 2D cuprates with elongated and tilted octahedral CuO_6 complexes as well as with the nonzero e_g splitting energy $\Delta_{\perp} = E_{B_{1g}} - E_{A_{1g}} > 0$, the pseudo-JT effect $(A_{1g} + B_{1g}) \otimes (b_{1g} + a_{1g})$ is possible [27]. The single-particle operators $c_{f\lambda\sigma}^{(+)}$ in the matrix elements (2) and quasiparticle transparency (3) are nondiagonal operators, and quenching effects can be expected.

As follows from Refs. [28,29] the phonons have zero thermal Hall response outside the pseudogap phase in the hole-doped 2D perovskite cuprates. However, inside the pseudogap phase, the phonons become chiral to generate the Hall response. They show the specific symmetric nature of the electron-lattice coupling. Next, we apply the MI criterion to understand the symmetric nature of phonons in the pseudogap effect of the hole spectrum in doped 2D perovskite cuprates. At first, we will test the MI criterion for doped cuprates in

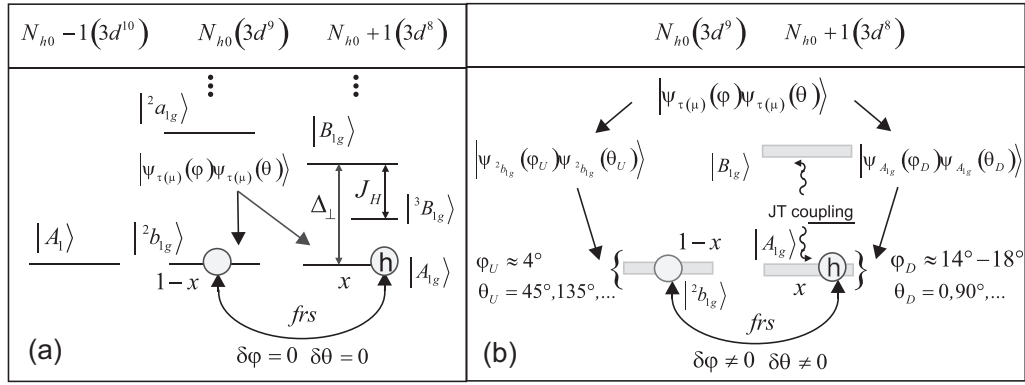


FIG. 3. $E_i(N_h, M_S)$ energy level scheme of the configuration space based on the cell states (15) in the CuO_2 layer. The solid line with arrows corresponds to the frs quasiparticles. (a) The tilting and orientation angles φ and θ of the CuO_6 octahedron are retained by the frs quasiparticles. (b) The wavy line shows the e_g states splitted by Δ_\perp energy, and active in the pseudo JT effect. The angles do not have specific magnitudes and they are changed by the frs quasiparticles.

the framework of the usual Russell-Saunders scheme. Let us calculate the magnitude of $N_{frs}^{s(r)}$ in the cuprates, where the root vector $r = \{^2b_1, A_{1g}\}$ is relevant in Eq. (A9) at $\mu = 0$ and $\tau = 0$ [30,31], i.e., it corresponds only to the A_{1g} singlet frs state, which is a well-known Zhang-Rice singlet [32]. Using the exact diagonalization procedure with the local density approximation (LDA) parameters from the work [33], we obtain the relation:

$$N_{frs}^s = 1 + [\beta_0^2(h_b) - \beta_0^2(h_{d_x})] \times [B_0^2(h_b^2) - B_0^2(h_{d_x}^2)] \approx 0.97 \quad (14)$$

for the singlet frs states, where the doublet and singlet ground states (5) and (6) are

$$\begin{aligned} |^2b_1\rangle_0 &= \beta_0(h_b)|h_b, \sigma_{\frac{1}{2}}\rangle + \beta_0(h_{d_x})|h_{d_x}, \sigma_{\frac{1}{2}}\rangle \\ |A_{1g}\rangle_0 &= B_0(h_b^2)|h_b^2, 0_0\rangle + B_0(h_{d_x}^2)|h_{d_x}^2, 0_0\rangle \\ &\quad + B_0(h_{d_x}, h_b)|h_{d_x}, h_b, 0_0\rangle, \end{aligned} \quad (15)$$

h_b and h_{d_x} are the holes in the b -symmetrized cell states of oxygen and $d_{x^2-y^2}$ cooper states of the CuO_2 layer, respectively. Thus, there is no l -forbidden quasiparticles in the Russell-Saunders scheme, and the number of valence states is almost a constant: $N_v(x) \approx N_e - 0.03x$. Here, the frs quasiparticles are associated with the single-hole transitions in Fig. 3(a), where the lattice of the CuO_2 layer is unchanged, and the adiabatic approximation is correct.

In the dynamic JT effect, the CuO_6 octahedra can be both in the U stripe, and D stripe states with different tilting and orientation angles $\varphi_{U(D)}$ and $\theta_{U(D)}$, respectively [27]. The hole concentration x in them is also different, and the dynamic JT effect in the CuO_2 layer as a whole would be possible only if its total charge and regular stripe structure were retained. Let us assume that the tilts $\varphi_{U(D)}$ and orientations $\theta_{U(D)}$ of the CuO_6 octahedra with respect to the spacer rock salt layers are active JT distortions, and the rotation of all the tilted CuO_6 octahedra around the c axis (i.e., changing their orientation θ) in the stripe U/D/U/D... structure fits within these limitations [34]. However, the scale of a novel JT cell in the stripe set U/D/U/D... exceeds the initial cell (i.e., the single CuO_6 octahedron). As a result, in the dynamic JT effect, the hole

number x is not retained in the single CuO_6 octahedron upon rotation around the c axis.

In Eqs. (2) and (3), where the matrix elements $\gamma_{\lambda\sigma}(r)$ were calculated still in the local Russell-Saunders scheme, there emerge overlapping phonon parts of the initial cell functions (A1) and (A2). According to the meaning, it is the Ham's reduction factor [35] in the quasiparticle transparency, since the JT cell has a fourfold degeneracy with different $\theta_{U(D)}$ orientations of the tilted CuO_6 octahedra:

$$\begin{aligned} \chi_{r_0 r_0}^\sigma(\delta\theta, \delta\varphi) \\ = \gamma_{x^2\sigma}^*(^1A_{1g}, ^2b_{1g})\gamma_{x^2\sigma}(^2b_{1g}, ^1A_{1g}) \cdot \sum_{\delta\varphi\delta\theta} \alpha(\delta\varphi, \delta\theta), \end{aligned} \quad (16)$$

where $r_0 = \{^1A_{1g}, ^2b_{1g}\}$, $\theta = \theta_U, \theta_D$ and $\varphi = \varphi_U, \varphi_D$ with the indices U and D related to the stripe affiliation for the single CuO_6 octahedron in the harmonic oscillator states $|\psi_{\tau(\mu)}(\theta)\rangle$ and $|\psi_{\tau(\mu)}(\varphi)\rangle$ of the displaced 2D oscillator [34]:

$$\begin{aligned} \alpha(\delta\varphi, \delta\theta) &= \langle\psi_{^1A_{1g}}(\theta_D)|\psi_{^2b_{1g}}(\theta_U)\rangle^2 \cdot \langle\psi_{^1A_{1g}}(\varphi_D)|\psi_{^2b_{1g}}(\varphi_U)\rangle^2 \\ &\approx \exp\{-v(\delta\theta^2 + \delta\varphi^2)/2\}, \end{aligned} \quad (17)$$

where $\delta\varphi = \varphi_D - \varphi_U \approx 9^\circ - 13^\circ$, $\delta\theta = \theta_D - \theta_U = \pm 45^\circ$ and $v = K/\hbar\omega_D$ with the Debye frequency ω_D and force coefficient K . Formally, the hole-doped 2D cuprate becomes an insulator only at $\omega_D \rightarrow 0$. We obtain the reduction effects in Eq. (17), if the charge inhomogeneity of the dynamical U/D/U/D... stripe structure [see Fig. 3(b)] occurs. To clarify the MI criterion itself and the last conclusion, we consider a simplified spinless model in Appendix B.

IV. CONCLUSIONS

According to Wilson's MI criterion for materials with strong electronic correlations, a class of the materials having the forbidden $frs(fes)$ quasiparticles in Hubbard gap was identified. In order to highlight the nature of the materials with specific single-particle excitations, but not two-particle excitations, we introduced the term "quasiparticle transparency" for the matrix element $\chi_{r_0 r_0}^\sigma$ [see Eq. (3)], which in these materials can have a zero magnitude, and the n or p doping does not lead

to the generation of charge carriers. Actually, by this term we note the analogy of the $frs(fes)$ quasiparticles with the light propagation in a material with optical intracell absorption at frequencies of the dd transitions. A first search for materials with low quasiparticle transparency allowed us to identify the following candidates:

(i) The doped $3d$ oxides with a spin crossover (e.g., n -doped FeBO_3 iron borate, $\text{Fe}_2\text{O}_3(3d^5)$, $\text{MnO}(3d^5)$, ... and p -doped $\text{LaCoO}_3(3d^6)$, $\text{Mg}_{1-x}\text{Fe}_x\text{O}$ magnesio wustite, ...), where the low quasiparticle transparency effects could be observed in the vicinity of the crossover at high pressure (e.g., $P_S = 48\text{--}54$ GPa for iron borate). The doped charge carriers are generated and disappear with increasing pressure. A possibility for the forbidden fes and frs quasiparticles is available only in n -doped materials with $3d^5$ and p -doped materials with $3d^6$ ions respectively. This is associated with a completely occupied t_{2g} shell of $3d$ ion in the octahedral environment, and materials with the local tetrahedral symmetry, such as spinels, must therefore be based on other $3d$ ions. Now, there is no information on the effects of low quasiparticle transparency in doped $3d$ oxides under high pressure. Missing data indicates complex detection. Indeed, a preliminary selection of the type (n or p) of doping for a specific material and low temperatures are required to occupy exclusively the $frs(fes)$ states.

(ii) The materials with the dynamic JT effect (2D perovskite cuprates), where overlapping phonon functions in different sectors N_{h0} and $N_{h0} + 1$ of the cell configuration space leads to a partial quenching of hole carriers. The essence of the quenching is that even in the dynamic JT effect, the doping holes avoid the U stripes, and the threshold nature of the pseudo JT effect at the doping concentration $x_D > x_c$ in the D stripes continues to support the charge inhomogeneous U/D/U/D... stripe structure. Otherwise, the hole concentration drops below critical $x < x_c$ and the pseudo-JT effect disappears [36]. However, the dynamic stripe structure is associated with the bifurcation nature of adiabatic potential for the tilted CuO_6 octahedra in Fig. 3(b). The prohibition on the $fes(frs)$ quasiparticle states is not the most effective there, because the crystal field corresponds to moderate magnitudes in the Cl-S-O-N-C ligand series. Indeed the prohibition is a property of structures with a specific crystal field, and the forbidden $frs(fes)$ states in rare earth materials are unlikely due to the shielded $4f$ orbitals. We also believe the complex layered spinel structure with octahedral and tetrahedral crystal fields, might be a promising example. In the chemistry of battery materials, the 3D spinel AM_2O_4 (A and M are the metal of the alkali group and $3d$ metal) can be obtained from some infinite layered structures of AMO_2 , through the intercalation process and the harmonious existence of complex layered spinel phases [37,38]. However, is the similar process possible for the infinite layer CaCuO_2 superconductor with a field effect doping [39,40]?

The real question is how can the doped materials with low quasiparticle transparency be identified? In undoped materials, the signatures of the forbidden $frs(fes)$ quasiparticles in the single-particle density of states are missing. However, they can be enhanced by a resonant optical excitation, since the condition for the zero magnitudes (2) does not apply to the optical matrix elements. Therefore, it is possible to detect

the low quasiparticle transparency by studying the difference between the optical gap and photoconductivity measurements for a mobility gap (see, e.g., Ref. [41]). The first corresponds to a charge transfer gap (the so-called a CT gap) in cuprates, where the light-induced frs “quasiparticles” are localized, and the second corresponds to a gap in spectrum of the charge carriers. As follows from our work, the difference in the undoped cuprates is directly related to the pseudogap effect in the hole-doped cuprates. The photoconductivity was mainly a topic of superconductor research in the 1990s, but the explanation for the effect is still under some debate [42].

In general, the angle resolved photoemission spectroscopy and observation of de Haas–van Alphen oscillations really show a hard gap in the density of states of the 2D cuprates [43,44]. However, Fermi arcs are observed in the k -dependent experiments at the nodal region of the 2D Fermi surface in a pseudogap state. It is impossible to interpret arcs within our approach, since there is no Fermi surface. The existence of Fermi arcs may be associated with limits of applicability of the MI criterion. Indeed in itinerant materials, the Wilson’s criterion is correct so long as the empty and occupied bands don’t overlap. The Mott-Hubbard material with the forbidden $frs(fes)$ quasiparticles can be in a dielectric state at some doping concentration in the range $0 < x < x_c$. Here, there is also restriction, since the overlapping bands with different root vectors $r = \{\mu, \tau\}$ changes a nature of the $frs(fes)$ states. In the 2D perovskite cuprates, the quasiparticle bands involving Zhang-Rice singlet $^1A_{1g}$ with $r = \{b_{1g}, ^1A_{1g}\}$ and triplet $^3B_{1g}$ with $r = \{b_{1g}, ^3B_{1g}\}$ can overlap [45,46] even at $W_{||}/\Delta_{\perp} < 1$, where $W_{||}$ is a width of the quasiparticle band in CuO_2 layer, due to the nonzero Hund exchange interaction $J_H \sim 0.1\text{eV}$ (see Fig. 3). In this case, the JT effect is impossible, and there is no prohibition from MI criterion at the broken condition $W_{||}/U < W_{||}/\Delta_{\perp} < 1$, i.e., for the doped Mott-Hubbard materials with overlapping bands.

ACKNOWLEDGMENT

This work has been supported by the grant of the Russian Science Foundation, RSF 22-22-00298.

APPENDIX A: THE NUMBER OF FRS(FES) STATES IN THE DOPED MOTT-HUBBARD MATERIALS

In the case of one hole per cell, the $|(N_h, M_S)_i\rangle$ cell states are a superposition of different hole configurations of the same orbital (l) symmetry:

$$|(N_{h0}, M_S)_\mu\rangle = \sum_{\lambda} \beta_{\mu}(h_{\lambda}) |h_{\lambda}, M_S\rangle |\psi_{\mu}(\varphi)\psi_{\mu}(\theta)\rangle. \quad (\text{A1})$$

Thus, there are $C_{2N_{\lambda}}^1 = 2N_{\lambda}$ one-hole spin doublet states, where C_n^k is the number of combinations. Altogether, there are $C_{2N_{\lambda}}^2 = N_S + 3N_T$ of the spin singlets $N_S = C_{N_{\lambda}}^2 + N_{\lambda}$ and triplets $N_T = C_{N_{\lambda}}^2$:

$$|(N_{h0} + 1, M'_{S'})_{\tau}\rangle = \sum_{v v'} B_{\tau}(h_v, h_{v'}) |h_v, h_{v'}, M'_{S'}\rangle \times |\psi_{\tau}(\varphi)\psi_{\tau}(\theta)\rangle \quad (\text{A2})$$

in the two-hole sector (see Fig. 1) of the N_λ orbital approach, where the harmonic oscillator wave function $|\psi_{\mu(\tau)}(\varphi)\psi_{\mu(\tau)}(\theta)\rangle = |\psi_{\mu(\tau)}(\varphi)\rangle|\psi_{\mu(\tau)}(\theta)\rangle$ associated with a (non)displaced 2D oscillator [34]. Using the intracell Hamiltonian H_0 in the cell function representation the configuration weights $\beta_\mu(h_\lambda)$ and $B_\tau(h_\lambda, h_{\lambda'})$ can be obtained by the exact diagonalization procedure for the matrices $(\hat{H}_0)_{\lambda\lambda'}$ and $(\hat{H}_0)_{\lambda\lambda'}^{v'}$ in the $E_i(N_h, M_S)$ -eigenvalue problem in different sectors N_h [10].

The sum (5) over all the r th excited states with $\mu \neq 0$ in the sector $N_h = N_{h0}$ is omitted, and only the excited states with any $\tau(\eta)$ index in the nearest $N_h = (N_{h0} + 1)$ and $(N_{h0} + 2)$ sectors are summed up. The expressions for the high- and low-spin two-hole partner states (with $S' = S \pm |\sigma|$) can be combined into a single expression:

$$|h_\lambda, h_{\lambda'}, M'_S\rangle = \left\{ \Gamma_\uparrow(S'_{M'}, S) c_{\lambda'\downarrow} |h_\lambda, M' - \frac{1}{2}\rangle + \text{sgn}(\Delta S) \Gamma_\downarrow(S'_{M'}, S) c_{\lambda'\uparrow} |h_\lambda, M' + \frac{1}{2}\rangle \right\}, \quad (\text{A3})$$

where $\Delta S = S' - S = \pm|\sigma|$, and the coefficients

$$\Gamma_\sigma^2(S'_{M'}, S) = \frac{S + \eta(\sigma) \text{sgn}(\Delta S) M' + \frac{1}{2}}{2S + 1} \quad (\text{A4})$$

have the completeness property for the contributions from the identical spin states of the doping hole to different high- and low-spin two-hole partners:

$$\sum_{\Delta S = -|\sigma|}^{+|\sigma|} \Gamma_\sigma^2(S'_{M'}, S) = \sum_\sigma \Gamma_\sigma^2(S'_{M'}, S) = 1, \quad (\text{A5})$$

and also

$$\sum_{M=-S}^S \Gamma_\sigma^2(S'_{M'}, S) = S + \frac{1}{2}. \quad (\text{A6})$$

Taking into account relations (A1), (A2), and (A6) we can determine the matrix element in Eq. (5) by the sum:

$$\langle (N_{h0} + 1, M'_S)_\tau | c_{v\sigma} | (N_{h0}, M_S)_\mu \rangle = \sum_{\lambda, \lambda', \lambda''} \langle h_{\lambda'}, h_{\lambda''}, M'_S | c_{v\sigma} | h_\lambda, M_S \rangle \beta_\mu(h_\lambda) B_\tau(h_\lambda, h_{\lambda'}) \Gamma_\sigma(S'_{M'}, S) \langle \psi_\tau(\varphi) \psi_\tau(\theta) | \psi_\mu(\varphi) \psi_\mu(\theta) \rangle. \quad (\text{A7})$$

After substituting Green's function (1), expressions (2) and (A6) in Eq. (5) we obtain:

$$N_v(x) = N_v^{12} + N_v^{23} = N_{s,v}^{12} + 3N_{t,v}^{12} + N_v^{23}, \quad (\text{A8})$$

where instead of the sum over the root vectors r , we used the summation over the physically meaningful indices τ , M and ΔS (i.e., the sum over all the low (s) and high (t) spin two-hole states). Here,

$$N_{s(t),v}^{12} = \sum_{v\sigma} \sum_\tau F_{r=(0,\tau)}^{s(t)}(x) \sum_{MM'} \left\{ \sum_\lambda \Gamma_\sigma(S'_{M'}, S) \beta_{\mu=0}(h_\lambda) B_\tau(h_\lambda, h_v) \delta(S', S \pm |\sigma|) \delta(M', M + \sigma) \right\}^2 \times \sum_{\varphi\theta} \langle \psi_\tau(\varphi) \psi_\tau(\theta) | \psi_{\mu=0}(\varphi) \psi_{\mu=0}(\theta) \rangle^2, \quad (\text{A9})$$

where (+) and (−) on the right side are used with the indices t and s , respectively, and the occupation factor in the PM phase

$$F_{(0,\tau)}^{s(t)}(x) = \begin{cases} \frac{1}{2}(1 - \alpha_{s(t)}x), & \tau = 0 \\ \frac{1}{2}(1 - x), & \tau \neq 0 \end{cases}, \quad (\text{A10})$$

with $\alpha_{s(t)} = 1 - 2/(2S' + 1)$ and $S' = 0, 1$; $S = 1/2$. Let us start with the contribution from the spin singlet frs states N_{frs}^s :

$$N_v(x) = (2N_\lambda - 1) - x(1 - N_{\text{frs}}^s) = N_e - x(1 - N_{\text{frs}}^s), \quad (\text{A11})$$

where the low and high spin contributions are

$$N_{s,v}^{12} = (1/2)[(N_\lambda + 1)(1 - x) + 2xN_{\text{frs}}^s] \quad (\text{A12})$$

and

$$N_{t,v}^{12} = (1/2)(N_\lambda - 1)(1 - x), \quad (\text{A13})$$

respectively. In the static case,

$$\sum_{\varphi\theta} \langle \psi_\tau(\varphi) \psi_\tau(\theta) | \psi_\mu(\varphi) \psi_\mu(\theta) \rangle^2 = \langle \psi_\tau(\varphi_{U,D}) \psi_\tau(\theta_{U,D}) | \psi_\mu(\varphi_{U,D}) \psi_\mu(\theta_{U,D}) \rangle^2 = 1, \quad (\text{A14})$$

at any $|\tau\rangle$ and $|\mu\rangle$ electron states since the tilting $\varphi = \varphi_{U,D}$ and orientation $\theta = \theta_{U,D}$ angles are fixed and associated with the minimum of the single adiabatic potential in the U and D stripes. The relation $N_v^{23} = x(2N_\lambda - 2)$ for the contributions from the quasiparticles with the root vectors from the $\{r_{23}\}$ subspace is derived similarly to the previous expression for contribution (A9). The number of possible singlet frs states is in the range $0 \leq N_{\text{frs}}^s \leq 2$, where

$$N_{\text{frs}}^s = 1 - \sum_\lambda \beta_0^2(h_\lambda) \sum_{\lambda', \lambda''} [1 - \delta_{\lambda\lambda'} - \delta_{\lambda\lambda''}] B_{\tau=0}^2(h_\lambda, h_{\lambda''}), \quad (\text{A15})$$

and $\tau = 0$ corresponds to the *frs*-quasiparticles. In deriving Eq. (A11) we also used Eq.(A6) and the identity $\sum_{\lambda} \beta_{\mu}^2(h_{\lambda}) \sum_{\lambda', \lambda''} B_{\tau}^2(h_{\lambda'} h_{\lambda''}) = 1$ at any μ and τ . Since the sum

$$\sum_{\tau} [\beta_0(h_{\lambda}) B_{\tau}(h_{\lambda}, h_{\nu})][\beta_0(h_{\lambda'}) B_{\tau}(h_{\lambda'}, h_{\nu})] = 0 \quad (\text{A16})$$

at any ν and $\lambda \neq \lambda'$, the contribution from the cross-term from Eq. (A9) to the total number of the valence states is missing. In the case of the triplet nature of the *frs* states, we obtain an expression similar to Eq. (A11) with the contribution

$$N_{\text{frs}}^t = 1 - \sum_{\lambda} \beta_0^2(h_{\lambda}) \sum_{\lambda' \neq \lambda'' \neq \lambda} B_{\tau=0}^2(h_{\lambda'} h_{\lambda''}), \quad (\text{A17})$$

where $0 \leq N_{\text{frs}}^t \leq 1$.

APPENDIX B: THE NUMBER OF FRS STATES IN THE DOPED MOTT-HUBBARD MATERIALS WITH THE PSEUDO-JT EFFECT

To show the role of the charge inhomogeneity, we obtain the MI criterion in a more simple three-orbital model ($\lambda = a, b, c$) of a semiconductor with two spinless electrons and hole doping $N_e = 2 - x$. Here, $|\mu\rangle = a_{\mu}|a\rangle + b_{\mu}|b\rangle + c_{\mu}|c\rangle$ and $|\tau\rangle = (ab)_{\tau}|a\rangle + (bc)_{\tau}|b\rangle + (ac)_{\tau}|c\rangle$, where $|\mu\rangle$ and $|\tau\rangle$ are the states with $\mu(\tau) = 0 - 2$ in the sectors N_{h0} and $N_{h0} + 1$, respectively. The coefficients satisfy the completeness relations $a_{\mu}^2 + b_{\mu}^2 + c_{\mu}^2 = 1$ and $(ab)_{\tau}^2 + (bc)_{\tau}^2 + (ac)_{\tau}^2 = 1$. In the homogeneous undoped case ($x = 0$), the number of valence states

$$N_v = N_v^{12} = \sum_{\tau} \{1 - a^2(bc)_{\tau}^2 - b^2(ac)_{\tau}^2 - c^2(ab)_{\tau}^2\} = 2, \quad (\text{B1})$$

since $\sum_{\tau} (bc)_{\tau}^2 = \sum_{\tau} (ab)_{\tau}^2 = \sum_{\tau} (ac)_{\tau}^2 = 1$, and thus, the material, according to the criterion, is a semiconductor, at $N_e = 2$. Now let $x \neq 0$, then,

$$\begin{aligned} N_v(x) &= N_v^{12} + N_v^{23} \\ &= N_{\text{frs}} + (1-x) \sum_{\tau=1}^2 \{1 - a_0^2(bc)_{\tau}^2 - b_0^2(ac)_{\tau}^2 - c_0^2(ab)_{\tau}^2\} \\ &\quad + N_v^{23} = 2 - \{1 - N_{\text{frs}}\}x, \end{aligned} \quad (\text{B2})$$

where $N_{\text{frs}} = 1 - a_0^2(bc)_0^2 - b_0^2(ac)_0^2 - c_0^2(ab)_0^2$, and $N_v^{23} = x$.

Now let us introduce into this model the JT instability in the two-particle sector, as is assumed for cuprates [34], where the JT distortions are the tilting and orientation angles φ and θ of the CuO_6 octahedra. In the dynamic state, all the octahedra do not have specific tilts φ and orientations θ , and all the states $|\tau(\mu)\rangle|\psi_{\mu(\tau)}(\varphi)\psi_{\mu(\tau)}(\theta)\rangle$ cannot be occupied with the factors $(1-x)$ and x in both sectors N_{h0} and $N_{h0} + 1$ of the configuration space. Indeed, in this case the charge inhomogeneity disappears along with the pseudo-JT effect at a concentration below the threshold $x < x_c$ [47,48]. We can choose the bifurcation potential in Fig. 3(b), at which a certain number x of the doped carriers still avoid the U stripes so that the number of valence states at $x \neq 0$ is

$$N_v(x) \approx 2 - \{1 - N_{\text{frs}}\}x \cdot \alpha(\delta\varphi, \delta\theta), \quad (\text{B3})$$

where

$$\begin{aligned} \alpha(\delta\varphi, \delta\theta) &= \sum_{\varphi_D \theta_D} \sum_{\varphi_U \theta_U} \langle \psi_{\mu=0}(\varphi_D) \psi_{\mu=0}(\theta_D) | \psi_{\tau=0}(\varphi_U) \psi_{\tau=0}(\theta_U) \rangle^2 \\ &\leq 1, \end{aligned} \quad (\text{B4})$$

and the number of valence states $N_v(x)$ decreases. Depending on the magnitude of $\alpha(\delta\varphi, \delta\theta)$, the criterion can detect the ground state of the doped JT material close to insulating one.

-
- [1] Y. Kohsaka, C. Taylor, P. Wahl, A. Schmidt, J. Lee, K. Fujita, J. W. Alldredge, K. McElroy, J. Lee, H. Eisaki, S. Uchida, D.-H. Lee, and J. C. Davis, *Nature (London)* **454**, 1072 (2008).
- [2] H.-B. Yang, J. D. Rameau, P. D. Johnson, T. Valla, A. Tsvetlik, and G. D. Gu, *Nature (London)* **456**, 77 (2008).
- [3] T. Saitoh, D. S. Dessau, Y. Moritomo, T. Kimura, Y. Tokura, and N. Hamada, *Phys. Rev. B* **62**, 1039 (2000).
- [4] N. Mannella, W. Yang, X. J. Zhou, H. Zheng, J. F. Mitchell, J. Zaanen, T. Devereaux, N. Nagasosa, Z. Hussain, and Z.-X. Shen, *Nature (London)* **438**, 474 (2005).
- [5] J. Hubbard, *Proc. R. Soc. A* **276**, 238 (1963).
- [6] A. H. Wilson, *Proc. R. Soc. A* **133**, 458 (1931).
- [7] V. A. Gavrichkov, *Solid State Commun.* **208**, 11 (2015).
- [8] G. S. Krinchik and M. V. Chetkin, *Sov. Phys. Usp.* **12**, 307 (1969).
- [9] V. V. Eremin and A. I. Belyaeva, *Sov. Phys. Usp.* **12**, 320 (1969).
- [10] S. G. Ovchinnikov, V. A. Gavrichkov, M. M. Korshunov, and E. I. Shneyder, *LDA+GTB Method for Band Structure Calculations in the Strongly Correlated Materials*, Springer Series in Solid-State Sciences (Springer, Berlin, 2011), Vol. 171, pp. 143–171.
- [11] Y. Tanabe and S. Sugano, *J. Phys. Soc. Jpn.* **11**, 864 (1956).
- [12] I. S. Lyubutin and A. G. Gavrilukin, *Phys. Usp.* **52**, 989 (2009).
- [13] V. A. Gavrichkov, S. I. Polukeev, and S. G. Ovchinnikov, *Phys. Rev. B* **101**, 094409 (2020).
- [14] G. J. Halder, C. J. Kepert, B. J. Moubaraki, K. S. Murray, and J. D. Cashion, *Science* **298**, 1762 (2002).
- [15] S. Ohkoshi, K. Imoto, Y. Tsunobuchi, S. Takano, and H. Tokoro, *Nat. Chem.* **3**, 564 (2011).
- [16] R. M. Wentzcovitch, J. F. Justo, Z. Wu, C. R. S. da Silva, D. A. Yuen, and D. Kohlstedt, *Proc. Natl. Acad. Sci. USA* **106**, 8447 (2009).
- [17] H. Hsu, K. Umamoto, Z. Wu, and R. M. Wentzcovitch, *Rev. Mineral. Geochem.* **71**, 169 (2010).
- [18] J. Liu, J. F. Lin, Z. Mao, and V. B. Prakapenka, *Am. Mineral.* **99**, 84 (2014).
- [19] R. Sinmyo, C. McCammon, and L. Dubrovinsky, *Am. Mineral.* **102**, 1263 (2017).

- [20] A. Marbeuf, S. Matar, P. Negrier, L. Kabalan, J. F. Letard, and P. Guionneau, *Chem. Phys.* **420**, 25 (2013).
- [21] M. Nishino, K. Boukheddaden, Y. Konishi, and S. Miyashita, *Phys. Rev. Lett.* **98**, 247203 (2007).
- [22] S. Ovchinnikov and V. N. Zabluda, *J. Exp. Theor. Phys.* **98**, 135 (2004).
- [23] T. Saha-Dasgupta and P. M. Oppeneer, *MRS Bull.* **39**, 614 (2014).
- [24] Y. V. Knyazev, N. V. Kazak, V. A. Gavrichkov, S. I. Polukeev, and S. G. Ovchinnikov, *JETP Lett.* **116**, 567 (2022).
- [25] S. G. Ovchinnikov, *J. Exp. Theor. Phys.* **107**, 140 (2008).
- [26] S. G. Ovchinnikov, *J. Exp. Theor. Phys.* **116**, 123 (2013).
- [27] V. A. Gavrichkov, Y. Shan'ko, N. G. Zamkova, and A. Bianconi, *J. Phys. Chem. Lett.* **10**, 1840 (2019).
- [28] G. Grissonnanche, S. Thériault, A. Gourgout, M. E. Boulanger, E. Lefrançois, Eois, A. Ataei, F. Laliberte, M. Dion, J. S. Zhou, S. Pyon, T. Takayama, H. Takagi, N. Doiron-leyraud, and L. Taillefer, *Nat. Phys.* **16**, 1108 (2020).
- [29] G. Grissonnanche, A. Legros, S. Badoux, E. Lefrançois, V. Zlatko, M. Lizaïre, F. Laliberte, A. Gourgout, J.-S. Zhou, S. Pyon, T. Takayama, H. Takagi, S. Ono, N. Doiron-leyraud, and L. Taillefer, *Nature (London)* **571**, 376 (2019).
- [30] L. F. Feiner, J. H. Jefferson, and R. Raimondi, *Phys. Rev. B* **53**, 8751 (1996).
- [31] V. A. Gavrichkov, A. A. Borisov, and S. G. Ovchinnikov, *Phys. Rev. B* **64**, 235124 (2001).
- [32] F. C. Zhang and T. M. Rice, *Phys. Rev. B* **37**, 3759 (1988).
- [33] M. M. Korshunov, V. A. Gavrichkov, S. G. Ovchinnikov, I. A. Nekrasov, Z. V. Pchelkina, and V. I. Anisimov, *Phys. Rev. B* **72**, 165104 (2005).
- [34] V. A. Gavrichkov and S. I. Polukeev, *Condens. Matter* **7**, 57 (2022).
- [35] F. S. Ham, *Phys. Rev.* **138**, A1727 (1965).
- [36] V. A. Gavrichkov, *Phys. B* **673**, 415457 (2024).
- [37] R. J. Clément, P. G. Bruce, and C. P. Grey, *J. Electrochem. Soc.* **162**, A2589 (2015).
- [38] T. Zhao, N. Zhou, X. Zhang, Q. Xue, Y. Wang, M. Yang, L. Li, and R. Chen, *ACS Omega* **2**, 5601 (2017).
- [39] M. Azuma, Z. Hiroi, M. Takano, Y. Bando, and T. Y., *Nature (London)* **356**, 775 (1992).
- [40] J. H. Schon, M. Dorget, F. C. Beuran, X. Z. Zu, E. Arushanov, C. D. Cavellin, and M. Lagues, *Nature (London)* **414**, 434 (2001).
- [41] G. Yu, C. H. Lee, A. J. Heeger, and S. W. Cheong, *Physica C* **203**, 419 (1992).
- [42] D. Destraz, Master's thesis, Physik-Institut Faculty of Science University of Zurich, 2015.
- [43] M. Hartstein, Y. Hsu, K. A. Modic, J. Porras, T. Loew, M. LeTacon, H. Zuo, J. Wang, Z. Zhu, M. K. Chan, R. D. McDonald, G. G. Lonzarich, B. Keimer, S. E. Sebastian, and N. Harrison, *Nat. Phys.* **16**, 841 (2020).
- [44] A. Kanigel, M. R. Norman, M. Randeria, U. Chatterjee, S. Souma, A. Kaminski, H. M. Fretwell, S. Rozenkranz, M. Shi, T. Sato, T. Takahashi, Z. Z. Li, H. Raffy, K. Kadowaki, D. Hinks, L. Ozyuzer, and J. C. Campuzano, *Nat. Phys.* **2**, 447 (2006).
- [45] H. Kamimura and M. Eto, *J. Phys. Soc. Jpn.* **59**, 3053 (1990).
- [46] M. Eto and H. Kamimura, *Physica C: Supercond.* **185-189**, 1599 (1991).
- [47] A. Bianconi, G. Bianconi, S. Caprara, D. Di Castro, H. Oyanagi, and N. Saini, *J. Phys.: Condens. Matter* **12**, 10655 (2000).
- [48] A. Bussmann-Holder, H. Keller, and K. A. Müller, *Superconductivity in Complex Systems* (Springer, Berlin, 2005), pp. 365–384.